Characterizing the structure of styrene-maleic acid copolymer-lipid nanoparticles (SMALPs) using RAFT polymerization for membrane protein spectroscopic studies

Benjamin D. Harding, **Gunjan Dixit**, **Kevin M. Burridge**, **Indra D. Sahu**, **Carole Dabney-Smith**, **Richard E. Edelmann**, **Dominik Konkolewicz**[*], and **Gary A. Lorigan**[*]

Department of Chemistry and Biochemistry, Miami University, 651 E. High Street, Oxford, Ohio 45056, United States

Abstract

Membrane proteins play an important role in maintaining the structure and physiology of an organism. Despite their significance, spectroscopic studies involving membrane proteins remain challenging due to the difficulties in mimicking their native lipid bilayer environment. Membrane mimetic systems such as detergent micelles, liposomes, bicelles, nanodiscs, lipodisqs have improved the solubility and folding properties of the membrane proteins for structural studies, however, each mimetic system suffers from its own limitations. In this study, using three different lipid environments, vesicles were titrated with styrene-maleic acid (StMA) copolymer leading to a homogeneous SMALP system (~10 nm) at a weight ratio of 1:1.5 (vesicle: StMA solution). A combination of Dynamic Light Scattering (DLS) and Transmission Electron Microscopy (TEM) was used to characterize these SMALPs. We used a controlled synthesis mechanism to synthesize StMA based block copolymers called reversible addition-fragmentation chain transfer polymerization (RAFT) SMALPs. Incorporation of the Voltage sensor Domain of KCNQ1 (Q1-VSD) into RAFT SMALPs indicates that this is a promising application of this system to study membrane proteins using different biophysical techniques. V165C in Q1-VSD corresponding to the hydrophobic region was incorporated into the SMALP system. Continuous Wave-Electron Paramagnetic Resonance (CW-EPR) line shape analysis showed line shape broadening, exposing a lower rigid component and a faster component of the spin label.

Keywords

[*]**Correspondence:** 1) Gary A. Lorigan, gary.lorigan@miamioh.edu, phone: (513)529-2813, fax: (513)529-5715; 2) Dominik Konkolewicz, d.konkolewicz@miamioh.edu, phone: (513)529-4395, fax: (513)529-5715.

1. Introduction

Membrane proteins make up almost 1/3 of total proteins and are responsible for various structural and functional properties of biological systems like transport of ions across membranes, receptors affecting down-stream signaling pathways and structure and assembly of the cells, thereby making them ideal drug targets[1–3]. However, the challenging task of mimicking the native membrane environment makes it extremely difficult to study membrane proteins using biophysical techniques.

Detergent micelles are the most common membrane mimetic system to solubilize membrane proteins for structural studies using high-resolution solution nuclear magnetic resonance (NMR) spectroscopy[4]. The structure of a membrane protein varies considerably from micelle to membrane bound environment (e.g. bicelles, liposomes, nanodiscs)[5–9]. Membrane mimetics, such as lipodisq nanoparticles and membrane scaffold protein (MSP)-stabilized nanodiscs, styrene-maleimide copolymer-lipid nanoparticles (SMILPs), and styrene-maleic acid copolymer-lipid nanoparticles (SMALPs) have been shown to enhance the accuracy of biophysical studies compared to previous membrane mimetic systems[8–14]. However, there are advantages and drawbacks to each of these mimetic systems[15]. Recent studies on the modified version of styrene-maleic acid copolymers have shown ultra-stability of monodispersed lipid bilayer nanodics[16]. Although liposomes are a widely accepted membrane mimetic system, they tend to form heterogeneous aggregates. Protein incorporation into these proves to be extremely difficult and often leads to misfolded proteins[17,18]. The spherical geometry of liposomes also makes it difficult to examine the cytoplasmic regions of trans-membrane proteins[19]. A popular membrane mimetic system is called bicelles and is composed of long-chained phospholipids and short-chained phospholipids, such as 1,2-Dimyristoyl-sn-glycero-3-phosphocholine (DMPC) and 1,2-diheptanoyl-sn-glycero-3-phosphocholine (DHPC). Bicelles form a disc-shape that allows biophysical techniques to probe the cytoplasmic region, hydrophobic interior of the lipid bilayer and extracellular region of the transmembrane protein[20–22]. However, bicelles can be only formed using limited phospholipid combinations, which may not be able to accommodate a native environment for many membrane proteins[19,23–24]. Nanodiscs, composed of a scaffold protein wrapped around a bundle of phospholipids, have proven to be advantageous. Nanodiscs can result from several types of phospholipid combinations, while the scaffold protein stabilizes the lipids and protein of interest[25,26]. Nanodiscs allow for more accurate biophysical analysis of membrane proteins that require specific types of lipids when compared to the limited combination of lipids that bicelles offer[26,27]. However, formation of nanodiscs is a detergent-based technique, which may distort the structure of the protein. The stabilizing scaffold protein's absorbance properties have also proven to interfere with the membrane protein to be studied[9,25]. Using polymers to form nanoparticles has proven to hold more advantages than scaffold protein nanodiscs[15]. Polymers such as styrene maleimide copolymer-lipid nanoparticles (SMILPs) and styrene-maleic acid copolymer-lipid nanoparticles (SMALPs) can solubilize the protein of interest without the use of detergent. SMALPs and SMILPs form nearly homogenous nanoparticles and provide a native mimicking environment with lipids that are compatible with the protein of interest, while stabilizing the protein with minimal interference[15,28].

Recent studies have used polymers to form membrane mimetic systems[14,15,28] and commercial polymers have been used to characterize the formation of lipodisq nanoparticles using dynamic light scattering (DLS), [31]P Solid State Nuclear Magnetic Resonance (SSNMR), and Transmission Electron Microscopy (TEM)[29]. Recently, our lab has shown that 3:1 styrene-maleic acid can be synthesized in a laboratory setting using reversible addition-fragmentation chain transfer polymerization (RAFT) polymerization and successfully used to characterize the structure of styrene-maleic acid copolymerlipid nanoparticles (SMALPs)[15,30]. RAFT polymerization is synthetically simple and provides flexibility to vary the structure of the polymer and influence the size of SMALPs[15,30]. SMALPs show compelling evidence that they are suitable for membrane protein incorporation[15].

In this study, we used SMALPs synthesized from commercial styrene-maleic acid (StMA) units. StMA was titrated with 1-palmitoyl-2-oleoyl-glycero-3-phosphocholine and 1-palmitoyl-2-oleoyl-sn-glycero-3-phospho-(1'-rac-glycerol) (POPC/POPG) vesicles and characterized using Dynamic Light Scattering (DLS), and Transmission Electron Microscopy (TEM) showing that a weight ratio of 1:1.5 resulted in a homogeneous lipid nanoparticle system. This SMALP system (1:1.5) was used to incorporate the Voltage Sensor Domain (Q1-VSD) of an integral membrane protein KCNQ1. Valine 165 in the trans-membrane segment of helix 2 of Q1-VSD was mutated to cysteine (V165C) and labeled with S-(1-oxyyl-2,2,5,5-tetramethyl-2,5-dihydro-1H-pyrrol-3-yl)methyl methanesulfonothioate (MTSL) spin labeling agent to make it EPR active for the studies using CW-EPR spectroscopy. KCNQ1 is a voltage-gated potassium channel protein with six transmembrane helices (S1–S6), involved in regulating the flow of potassium ions in the heart and composed of the voltage sensor domain, Q1-VSD (S1–S4), and the pore domain (S5–S6)[31,32]. CW-EPR spectra revealed higher side chain mobility in liposomes when compared to SMALPs consistent with previous studies[10].

2. Materials and Methods

2.1 Typical Synthesis of a One-pot Block Copolymer of Poly(styrene-alt-maleic anhydride-b-styrene)

All materials were obtained from commercial suppliers and used as received unless otherwise specified. The synthesis of poly(styrene-alt-maleic anhydride-b-styrene) was carried out as an adaptation of a previously described procedure[15,33]. Briefly, Styrene (3.6608 g, 35.1 mM), Maleic Anhydride (0.98 g, 10 mM), and 2-(Dodecylthiocarbonothioylthio)propionic acid (PADTC) (0.1404 g, 0.4 mM) were combined in a 20 mL vial and dissolved in 4.64 g 1,4-dioxane. 1,1-Azobis(cyclohexanecarbonitrile) (ACHN) (0.0195 g, 0.008 mM) was added and dissolved. The contents of the vial were transferred to a 50 mL round bottom flask with a magnetic stir bar and small aliquot of solution was set aside. The flask was capped with a rubber stopper and bubbled with nitrogen for 15 minutes. The solution was heated to 90 °C for 20 hours. Once comparison by NMR with the previously set aside aliquot showed sufficient conversion (~80%), the polymer was purified by 3 sequential precipitations from tetrahydrofuran (THF) into a large excess of cold hexanes, yielding 4 g of yellow powder.

2.2 End-group Removal of Poly(styrene-alt-maleic anhydride-b-styrene)

The polymer (ca. 4 g) was dissolved in dioxane and combined with 2.4 g of benzoyl peroxide (9.9 mM) in a 50 ml round bottom flask. The flask was sealed with a rubber stopper and bubbled with nitrogen for 15 minutes. The escape needle was left in the flask and the flask was heated to 82 °C for 5 hours. Upon completion, the polymer was precipitated twice from THF into a large excess of cold hexanes, yielding a white to off-white powder.

2.3 Hydrolysis of 3:1 Styrene-maleic Anhydride

The anhydride moieties of the polymer were hydrolyzed using NaOH to their succinic acid counterparts as previously described[15] with slight modifications. Briefly, equal mass of polymer and THF (1 g) were combined in a vial, and briefly heated to 95 °C while swirling to dissolve all the polymer. Then, a 4x molar excess of aqueous 2 M NaOH was added dropwise while stirring, and the resulting mixture was heated at 65 °C for 24 hours. Another 10 mL of distilled water was added, and the mixture was heated for another 24 hours. At the end of this period, the solution is stable at room temperature. The THF and excess base were removed by dialysis in 3.5 kDa cutoff tubing, using two 1 L portions of ultrapure water. The polymer was collected in a 50 mL conical tube and frozen in a −80 °C refrigerator overnight, then lyophilized, yielding a white to off-white powder. The NMR data on the hydrolyzed polymer is shown in the supporting information in Figure S1. The NMR peaks corresponding to styrene aromatic protons are observed in the 6.0 – 7.5 ppm region of the spectrum. To the best of our knowledge, precise NMR characterization of these copolymers has not been done. This is mainly due to the significant broadening observed when the maleic anhydride protons are incorporated into the polymer backbone. Hence a meaningful resolution of these protons cannot be obtained. These RAFT-synthesized copolymers are characterized by a much steeper gradient, as opposed to block copolymers.

2.4 Size Exclusion Chromatography (SEC) Procedure

5 mg of polymer was dissolved in 1.5 mL THF with 0.025% butylated hydroxy toluene (BHT). Two drops of toluene were added as a flow rate marker. The solution was then filtered through a 0.22 μm filter. Size exclusion chromatography was performed using an Agilent 1260 gel permeation chromatography system coupled with an autosampler, a guard and 2× PL Gel Mixed B columns, and a refractive index detector. The eluent was tetrahydrofuran running at 1 mL/min at 25 °C. The system was calibrated with poly(methyl methacrylate) standards in the range of 617,000 to 1010 and corrected to polystyrene using the standard Mark-Houwink parameters $K_{MMA} = 12.8$, $\alpha_{MMA} = 0.69$, $K_{Sty} = 11.4$, $\alpha_{Sty} = 0.716$. The M_n by GPC, after applying the Mark-Houwink correction for polystyrene was 7.0kDa, M_w of 9.8kDa, with a polydispersity of 1.40. The molecular weight distribution data on the polymer are also included in the supporting information in Figure S2.

2.5 Vesicle Preparation and Formation of SMALPs

To characterize the formation of homogeneous SMALPs, two different lipids commonly used for studying membrane proteins were used. One vesicle sample was composed of POPC, another one was composed of a molar ratio of 3:1 (POPC:POPG) and the third

vesicle sample was composed of a molar ratio of 9:1 (POPC:POPG). In each of the samples, powdered lipids were dissolved in a 2-(4-(2-Hydroxyethyl)piperazin-1-yl)ethanesulfonic acid (HEPES) buffer (20 mM HEPES, 100 mM NaCl, pH 7.0) and brought to a final concentration of 25 mM. The mixture was then vortexed vigorously for one minute and followed by at least 15 freeze/sonication cycles (<30°C) to obtain a homogeneous milky solution. The vesicle solutions were then frozen with liquid nitrogen and placed in a freezer overnight (−20 °C). Dynamic light scattering was used to confirm and analyze the size of vesicles the next day.

Styrene-maleic acid was dissolved in a buffer (20mM HEPES, 100mM NaCl pH7), brought to a final concentration of 2.5% (m/v) and sonicated at 30–40 °C until the solution went clear. The vesicles (POPC, POPC/POPG) were titrated with StMA polymer by adding StMA solution dropwise obtaining the weight ratios of 1:0.5, 1:1, 1:1.25 and 1:1.5 (vesicles:StMA). The newly formed SMALP solution was mixed via slight rotation at room temperature overnight.

2.6 Preparation of Q1-VSD for CW-EPR Spectroscopic Study

The His-tag expression vector (pET-16b) containing wild type Q1-VSD (residues 100–249) was expressed and purified using Rosetta/C43(DE3) strain of *E.coli* as previously described[4]. Briefly, site-directed mutagenesis was performed to remove all the native cysteines and generate single cysteine mutants from the cys-less vector using the QuickChange Lightning Site-Directed Mutagenesis Kit (Stratagene). The mutation was confirmed by DNA sequencing and was transformed into Rosetta/C43(DE3) *E.coli* cells for protein overexpression.

The overexpression and purification of Rosetta/C43(DE3) *E. coli* cells carrying mutated Q1-VSD genes were carried out using a previously described protocol[4]. *E. coli* cells carrying mutant (V165C) was grown in an M9 minimal medium with 100 μg/mL ampicillin and 50 μg/ml chloramphenicol. The cell culture was incubated at 25 °C and 240 rpm supplemented with MEM vitamin (Mediatech) and $ZnCl_2$ (50 μM) until the OD_{600} reached 0.8, at which point protein expression was induced using 1 mM isopropyl-1-thio--D-galactopyranoside (IPTG), followed by continued rotary shaking at 25°C for 24 h. Purification of Q1-VSD from inclusion bodies was carried out according to a previously described method[4] and eluted using 0.1% 1-myristoyl-2-hydroxy-*sn*-glycero-3-phospho-(1'-*rac*-glycerol) (LMPG) detergent. Protein samples were concentrated using a Microcon YM-3 (molecular weight cutoff, 3,000) filter (Amicon). The protein concentration was measured with a nanodrop and purity was confirmed by SDS-PAGE. Spin labeling, and liposomes reconstitution was carried out following a similar protocol previously described[34]. After purification, cysteine mutant was concentrated to 0.5 mM. Sample was then reduced with 2.5 mM Dithiothreitol (DTT), with gentle agitation at room temperature for 24 hours to ensure complete conversion to Cys-SH. MTSL spin label was added to 10 mM from a 250 mM solution in methanol into 0.5 mM Q1-VSD solution, which was then equilibrated at room temperature for 30 minutes, followed by incubation at 37 °C for 3 hours and further incubated overnight at room temperature. Sample was then buffer-exchanged into a 50 mM phosphate, 0.1% LMPG, pH 7.8. Following buffer exchange, samples were bound to Nickel resin in a

column, which was then washed with 200 mL of 50 mM phosphate, 0.05% n-dodecylphosphocholine (DPC), pH 7.8 to remove excess MTSL. The spin labeled Q1-VSD was eluted using elusion buffer containing 0.5% DPC. The reconstitution of spin labeled protein into POPC/POPG (3:1) proteoliposomes was carried out via dialysis methods following a similar protocol in the literature[14]. The concentrated spin labeled Q1-VSD protein was mixed with stock lipid slurry (400 mM SDS, 75 mM POPC and 25 mM POPG, 0.1 mM ethylenediaminetetraacetic acid (EDTA), 100mM imidazole (IMD), pH 7.5). The lipid slurry was pre-equilibrated to clear mixed micelles via several freeze thaw cycles. The final protein:lipid molar ratio was set to 1:250. The Q1-VSD-lipid mixture was then subjected to extensive dialysis to remove all detergent present and help form Q1-VSD/POPC/POPG vesicles.

The protein-lipid complex was incorporated into SMA-polymer following previously published protocols[11,14]. A 500 μl aliquot of proteoliposome-reconstituted protein sample (~30 mM POPC/POPG lipid) was added with the 2.5% of StMA polymer solution prepared in the same dialysis buffer drop-wise over 3–4 minutes at a weight ratio 1:1.5. The protein-StMA-polymer solution was equilibrated overnight at 4 °C. The resulting solution was centrifuged at 40,000xg for 30 minutes to remove the nonsolubilized protein. The supernatant was further concentrated to desired volume and concentration for CW-EPR spectroscopic measurements.

2.7 Dynamic Light Scattering (DLS) Measurements

DLS measurements were performed on a ZETASIZER NANO Series (Malvern Instruments) at 25 °C in disposable 40 μL micro cuvettes. Data were collected for 20 s and averaged for 10 scans. The size distribution in radius is shown on a log scale using Igor Pro (WaveMetrics).

2.8 CW-EPR Measurements

EPR experiments were conducted at the Ohio Advanced EPR Laboratory. CW-EPR spectra were collected at X-band on a Bruker EMX CW-EPR spectrometer using an ER041xG microwave bridge and ER4119-HS cavity coupled with a BVT 3000 nitrogen gas temperature controller. Each spin-labeled CW-EPR spectrum was acquired by signal averaging 20 42-s field scans with a central field of 3315 G and sweep width of 100 G, modulation frequency of 100 kHz, modulation amplitude of 1 G, and microwave power of 10 mW at room temperature.

2.9 Transmission Electron Microscopy

One drop of control POPC/POPG vesicles and StMA-lipid nanoparticle (1/1.25) samples out in a solution of 100 mM NaCl, 20 mM HEPES pH 7.0 were adsorbed to 200 mesh copper carbon-coated grids for 10 s for full absorbance. The grids were stained with two drops of 1.5% ammonium molybdate. Images were recorded using JEOL-1200EX.

3.   Results and Discussion

Figure 1 shows the DLS data of POPC vesicles and the addition of 2.5% (m/v) RAFT StMA polymer solution. The varying ratios of StMA can be used to control the overall particle size as shown by previously published data[15] and was found to be consistent with this study. Figure 1A displays the DLS data for POPC vesicles indicating a unimodal peak with a wide size distribution representing heterogeneity in the sample. The heterogeneity of POPC vesicles was confirmed using TEM (Figure 2A). When these vesicles were titrated with a 2.5% StMA solution at a weight ratio of 1:0.5 (POPC:StMA), DLS data showed more heterogeneity as indicated by the wider size distribution as presented in Figure 1B. The addition of StMA possibly causes aggregation of the vesicle sample at this ratio. The sample at this weight ratio appeared to be mostly transparent, but some lipids remained visually undissolved. A ratio of 1:1 (POPC:StMA) shows a bimodal graph indicating two separate components in the sample as shown in Figure 1C. One component has a smaller size distribution of particles with the peak centered at 21 nm, while the other larger component showed a wider size distribution corresponding to an average particle size of 127 nm. The smaller size distribution of the first component is indicative of SMALP formation, while the larger size distribution in the second component indicates POPC vesicles in solution that have not solubilized with StMA. This mixture showed to be primarily transparent due to the solubilization of lipids by StMA. Figure 1D represents the 1:1.25 (POPC:StMA solution) ratio that shows a similar bimodal graph as Figure 1C. However, the first component with a smaller size distribution of particles in solution is depressed and slightly decreased with an average particle size of 18 nm, while the component with a larger size distribution of particles shows a decrease in the intensity, indicative of a decrease in the heterogeneity of the vesicles. The solution became visually transparent due to the solubilization of lipids. Finally, when the weight ratio of POPC to StMA solution was increased to 1:1.5, as shown in Figure 1E, DLS data showed one dominant peak with an average size distribution of 10 nm. The solution was also visually transparent at this stage. The homogeneity of the sample was confirmed using TEM as shown in Figure 2B[15,29]. This result is consistent with the previously published data[15].

Figure 3 shows the DLS data of 3:1 (POPC:POPG) titrated with the same 2.5% (m/v) StMA solution. Similar heterogeneity (reported above) was observed for 3:1 (POPC:POPG) vesicle sample as shown in Figure 3A with a relatively large size and the finding was confirmed using TEM[15,29] (Figure 4A). Vesicles were first titrated with the StMA at weight ratio of 1:0.5 (Figure 3B), resulting in a bimodal graph by DLS and a partially clear solution with some visible aggregation was still present. Although it showed a wide size distribution, it resulted in a 2-component peak. The more intense peak indicated SMALP formation due to the lower size distribution, while the less-intense peak replicates the unsolubilized vesicles shown in Figure 3A. Figure 3C reveals a weight ratio (vesicles:StMA) of 1:1 and showed improvements from the previous ratio of 1:0.5 with respect to the homogeneity and the clarity of the sample. At the weight ratio of 1:1, the solution became visually transparent. The data indicate two components; one with a relatively low size distribution of particles with the peak centered at 30 nm indicating that the StMA is beginning to solubilize the vesicles to form SMALPs; the component with a larger size distribution of particles similar

to vesicles (Figure 3A) remained in solution and indicates some nonsolubilized vesicles. As the 3:1 (POPC:POPG) vesicles were further titrated to a weight ratio of 1:1.25 (Figure 3D), StMA solubilizes the majority of the vesicles present as shown in Figure 3C and showed a visually transparent solution. The component with a smaller size distribution of the particles also decreased with an average particle size distribution of 30 nm. It can be inferred that as more polymer is added to the vesicles, the SMALP formation caused reduction; both in size itself and the size distribution and agrees with previous literature studies[15,29]. This is also observed as the vesicles are further titrated with 1:1.5 (vesicles:StMA solution) as shown in Figure 3E. At this ratio, the entire solution was clear and has fully solubilized the vesicles to form SMALPs with a decreased size distribution as indicated by the peak centered at 10 nm. The homogeneity of the SMALPs is further confirmed using TEM (Figure 4B).

Figure 5 shows the DLS data of 9:1 (POPC:POPG) vesicles. Vesicles were synthesized with a molar ratio of 9:1 (POPC:POPG) and titrated with 2.5% (m/v) StMA in buffer (20mM HEPES, 100mM NaCl pH7). Figure 5A presents the DLS data for 9:1 (POPC:POPG) vesicles. The vesicles show consistent data by providing a heterogeneous solution which is further confirmed using TEM as shown in Figure 6A. As StMA is further titrated with the 9:1 (POPC:POPG) vesicles to a 1:0.5 weight ratio (vesicles:StMA) as displayed in Figure 5B, a significant amount of StMA solubilizes the vesicles, but shows a small amount of aggregation. This is reflected in the DLS data as the dominant peak in the bimodal graph is further depressed and narrows down, which is a consistent trend of SMALP formation[15]. However, a portion of the solution showed a small peak indicative of the unsolubilized vesicles at a larger distance. Figure 5C shows the titration data of 1:1 (vesicles:StMA) with a slight improvement from the previous titration ratio of 1:0.5 and showed to be nonsolubilized. Although DLS generated a similar graph to that of Figure 5B, the dominant peak showed a downward shift as well as a decrease in size distribution, indicative that StMA is still solubilized with the vesicles to form a homogeneous SMALP system. As more StMA is added to a ratio of 1:1.25 (vesicles:StMA) as shown in Figure 5D, a majority of vesicles are solubilized by StMA to form homogeneous SMALPs as shown by the dominant peak with a size distribution of 10 nm, only a small portion of vesicles have not solubilized with StMA even though the sample remains visually transparent. Finally, a weight ratio of 1:1.5 (vesicles:StMA) was also completely clear and found to give the best data with the average size distribution of ~9 nm for completely homogeneous SMALPs and is presented in Figure 5E. The finding and size distribution were further confirmed using TEM as shown in Figure 6B.

As stated above, TEM was used to further confirm the data obtained from DLS experiments as DLS tends to be biased towards larger particle sizes[15,29]. Our TEM data is in good agreement with the DLS data obtained for different ratios of vesicles to StMA and clearly shows that at 2.5% StMA and a ratio of 1:1.5 (vesicles:StMA) we were able to obtain homogeneous SMALPs. Using the three titrations presented Figures 1, 3, and 5, SMALP systems were successfully characterized in different lipid environments at a critical weight ratio of 1:1.5. Table 1 presents the size distributions for each of the three titrations presented above. The data clearly indicates that the formation of SMALPs clearly works for a variety of phospholipids. Further investigation of StMA in the presence of other lipids will progress the study of membrane proteins in different lipid environments. For all the liposome samples

studied the addition of more StMA (upto 1:2) did not significantly reduce the size of the SMALPs.

Successful characterization of SMALPs in a 3:1 (POPC:POPG) environment was tested with the integral membrane protein Q1-VSD. Q1-VSD is composed of four trans-membrane helices[4]. To test the compatibility of the SMALP system and membrane proteins, residue V165C was spin-labeled and incorporated into 3:1 (POPC:POPG) vesicles and StMa solution was added until a weight ratio of the protein sample to StMA solution was 1:1.5. For all the liposome samples studied, the addition of more StMA (up to 1:2) did not significantly reduce the size the SMALPs. V165C is an amino acid mutant embedded in the second helix within the lipid bilayer of Q1-VSD. Spin labeled residue in a SMALP system versus spin labeled residue in a 3:1 vesicle environment (liposome) were compared using CW-EPR line shape analysis as displayed in Figure 7. The spin-labeled Q1-VSD V165C in the SMALP system showed line shape broadening, revealing two motional components signified by the two arrows. The left arrow shows the slow and more rigid component, while the right arrow points to the faster motional component of the spin label. These two components, however, are not present in the liposome. This data is consistent with previous studies of characterizing the membrane protein KCNE1 in the presence of lipodisq nanoparticles[10] clearly suggesting that the SMALP system is compatible with membrane proteins and allows for the analysis of membrane proteins using biophysical technique, such as CW-EPR spectroscopy.

4. Conclusion

Knowledge and research on SMALP systems is exponentially growing[10,15,29]. In this study, SMALPs were characterized by titrating different ratios of POPC:POPG with the RAFT synthesized StMA. The resulting homogeneous SMALP solution was found to have an average size of 10 nm. This newly synthesized RAFT SMALP system was used as a new membrane mimetic system to show successful incorporation of Q1-VSD membrane protein and analyzed using CW-EPR spectroscopy. Overall, our data suggests a promising future for this membrane mimetic system with a great potential for studies using biophysical techniques. RAFT SMALPs offer great potential in being synthetically simple, and economical alternative to other current membrane mimetic systems. It provides flexibility with the structure of the polymer and therefore better control on the size of SMALPs[15].

Acknowledgements

References

1. Hang Y, and Flynn AD, 2016 Drugging membrane protein interactions. Annu Rev Biomed 18, 51–76.

2. Bull SC, and Doig AJ, 2015 Properties of protein drug target classes. PLoS One, 10(3).

3. Overington JP, Al-Lazikani B, and Hopkins AL, 2006 How many drug targets are there? Nat Rev Drug Discovery 5, 993–996. [PubMed: 17139284]

4. Peng D, Kim JH, Kroncke BM, Law CL, Xia Y, Droege KD, Van Horn WD, Vanoye CG and Sanders CR 2014 Purification and structural study of the voltage-sensor domain of the human KCNQ1 potassium ion channel. Biochemistry 53, 2032–2042. [PubMed: 24606221]

5. Coey AT, Sahu ID, Gunasekera TS, Troxel KR, Hawn JM, Wickenheiser MR, Welch RC, Vanoye CG, Kang C, Sanders CR, and Lorigan GA, 2011 Reconstitution of KCNE1 into Lipid Bilayers: Structural and Dynamic Differences in Micelle and Vesicle Environments. Biochemistry 50, 10851–1085. [PubMed: 22085289]

6. Yu L, Wang W, Ling S, Liu S, Xiao L, Xin Y, Lai C, Xiong Y, Zhang L, and Tian C, 2015 CW-EPR studies revealed different motional properties and oligomeric states of the integrin β1a transmembrane domain in detergent micelles or liposomes. Scientific Reports 5, 7848. [PubMed: 25597475]

7. Seddon AM, Curnow P, and Booth PJ, 2004 Membrane proteins, lipids, and detergents: not just a soap opera. Biochim Biophys Acta 1666, 105–117. [PubMed: 15519311]

8. De Angelis AA, Nevzorov AA, Park SH, Howell SC, Mrse AA, and Opella SJ, 2004 High resolution NMR spectroscopy of membrane proteins in aligned bicelles. J Am Chem Soc 126, 15340–15341. [PubMed: 15563135]

9. Bayburt TH, and Sligar SG, 2003 Self-assembly of single integral membrane proteins into soluble nanoscale phospholipid bilayers. Protein Sci 12, 2476–2481. [PubMed: 14573860]

10. Sahu ID, Zhang R, Dungan MM, Craig AF, Lorigan GA, 2017 Characterization of KCNE1 inside lipodisq nanoparticles for EPR spectroscopic studies of membrane proteins. J Phys Chem, 121, 5312–5321.

11. Orwick MC, Judge PJ, Procek J, Lindholm L, Graziadei A, Engel A, Grobner G, and Watts A, 2012 Detergent free formation and physicochemical characterization of nanosized lipids-polymer complexes: lipodisq. Angew Chem, Int Ed. 51, 4653–4657.

12. Park SH, Opella SJ, 2012 TritonX-100 as the "short-chain lipid" improves the magnetic alignment and stability of membrane proteins in phosphatidylcholine bilayers for oriented-sample solid-state NMR spectroscopy. J. Am. Chem. Soc 132 (36) 12552–12553.

13. De Angelis AA, Opella SJ, 2007 Bicelle samples for solid-state NMR of membrane proteins. Nat. Protoc 2 (10), 2332–2338. [PubMed: 17947974]

14. Sahu ID, McCarrick RM, Troxel KR, Zhang R, Smith HJ, Dunagan MM, Swartz MS, Rajan PV, Kroncke BM, Sanders CR, Lorigan GA, 2013 DEER EPR measurements for membrane protein structures via bifunctional spin labels and lipodisq nanoparticles. Biochemistry 52 (38), 6627–6632. [PubMed: 23984855]

15. Craig AF, Clark EE, Sahu ID, Zhang R, Frantz ND, Al-Abdul-Wahid S, Dabney-Smith C, Konkolewicz D, Lorigan GA, 2016 Tuning the size of styrene-maleic acid copolymer-lipid nanoparticles (SMALPs) using RAFT polymerization for biophysical studies. Biochim. Biophys. Acta 1858, 2931–2939. [PubMed: 27539205]

16. Ravula T, Hardin NZ, Ramadugu SK, Cox SJ, Ramamoorthy A, 2018 Formation of pH-Resistant Monodispersed Polymer-Lipid Nanodiscs. Angew Chem, Int Ed. 57 (5), 1342–1345.

17. Geertsma ER, Mahmood NABN, Schuurman-Wolters GK, and Poolman B, 2008 Membrane reconstitution of ABC transporters and assays of translocator function. Nat. Protoc 3 (2), 256–266. [PubMed: 18274528]

18. Fang G, Friesen R, Lanfermeijer F, Hagting A, Poolman B, Konings WN, 1999 Manipulation of activity and orientation of membrane-reconstituted di-tripeptide transport protein DtpT of Lactococcus lactis. Mol. Membr. Biol 16 (4), 297–304. [PubMed: 10766129]

19. Raschle T, Hiller S, Etzkorn M, Wagner G, 2010 Nonmicellar systems for solution NMR spectroscopy of membrane proteins. Curr. Opin. Struct. Biol 20 (4), 471–479. [PubMed: 20570504]

20. Lau T-L, Kim C, Ginsberg MH, Ulmer TS, 2009 The structure of the integrin alpha IIb beta 3 transmembrane complex explains integrin transmembrane signaling. EMBO J. 28 (9), 1351–1361. [PubMed: 19279667]

21. Lee D, Walter KFA, Brueckner A-K, Hilty C, Becker S, Griesinger C, 2008 Bilayer in small bicelles revealed by lipid-protein interactions using NMR spectroscopy. J. Am. Chem. Soc 130 (42), 13822–13823. [PubMed: 18817394]

22. Sanders CR, Prosser RS, 1998 Bicelles: a model membrane system for all seasons? Structure 6 (10), 1227–1234. [PubMed: 9782059]

23. Vold RR, Prosser RS, 1996 Magnetically oriented phospholipid bilayered micelles for structural studies of polypeptides. Does the ideal bicelle exist? J. Magn. Reson. Ser. B 113 (3), 267–271.

24. Duerr UHN, Gildenberg M, Ramamoorthy A, 2012 The magic of bicelles lights up membrane protein structure. Chem. Rev 112 (11), 6054–6074. [PubMed: 22920148]

25. Bayburt TH, Sligar SG, 2010 Membrane protein assembly into nanodiscs. FEBS Lett. 584 (9), 1721–1727. [PubMed: 19836392]

26. Borch J, Hamann T, 2009 The nanodisc: a novel tool for membrane protein studies. Biol. Chem 390 (8), 805–814. [PubMed: 19453280]

27. Hagn F, Etzkorn M, Raschle T, Wagner G, 2013 Optimized phospholipid bilayer nanodiscs facilitate high-resolution structure determination of membrane proteins. J. Am. Chem. Soc 135 (5), 1919–1925. [PubMed: 23294159]

28. Hall SCL, Tognoloni C, Charlton J, Bragginton ÉC, Rothnie AJ, Sridhar P, Wheatley M, Knowles TJ, Arnold T, Elder KJ, Dafforn TA, 2018 An acid-compatible co-polymer for the solubilization of membranes and proteins into lipid bilayer-containing nanoparticles. Nanoscale (10), 10609–10619. [PubMed: 29845165]

29. Zhang R, Sahu ID, Liu L, Osatuke A, Comer RG, Dabney-Smith C, Lorigan GA, 2015 Characterizing the structure of lipodisq nanoparticles for membrane spectroscopic studies. Biochem. Biophys. Acta 329–333.

30. Smith AAA, Autzen HE, Laursen T, Wu V, Yen M, Hall A, Hansen SD, Cheng Y, and Xu T, 2017 Controlling styrene maleic acid lipid particles through RAFT. Biomacromolecules, 18, 3706–3713. [PubMed: 28934548]

31. Jespersen T, Grunnet M, Olesen SP, 2005 The KCNQ1 potassium channel: From gene to physiological function. Physiology, 20, 408–416. [PubMed: 16287990]

32. Sun J, and MacKinnon R, 2017 Cryo-EM structure of a KCNQ1/CaM complex reveals insights into congenital long QT syndrome. Cell 169, 1042–1050. [PubMed: 28575668]

33. Bapat AP, Ray JG, Savin DA, Hoff EA, Patton DL, Sumerlin BS, 2012 Dynamic-covalent nanostructures prepared by Diels-Alder reactions of styrene-maleic anhydride-derived copolymers obtained by one-step cascade block copolymerization. Polym. Chem-Uk 3 (11), 3112–3120.

34. Barrett PJ, Song Y, Van Horn WD, Hustedt EJ, Schafer JM, Hadziselimovic A, Beel AJ, Sanders CR, 2012 The Amyloid Precursor Protein Has a Flexible Transmembrane Domain and Binds Cholesterol. Science, 336 (6085)

Highlights:

- The size of styrene-maleic acid copolymer-lipid nanoparticles (SMALPs) were characterized using Dynamic Light Scattering.

- EPR spectra showed the incorporation of a membrane protein into the nanoparticles and liposomes.

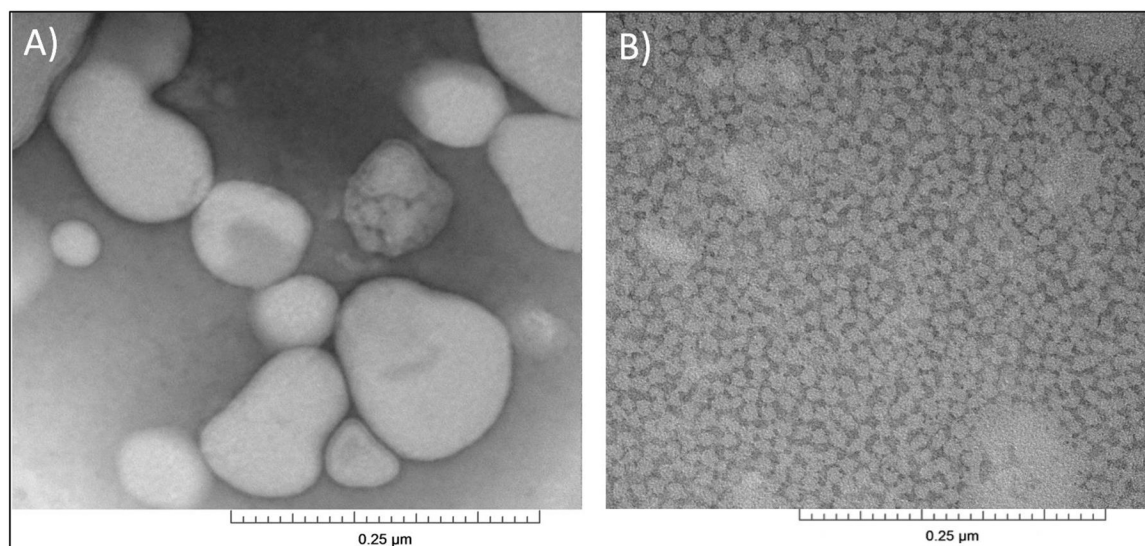- TEM images show the size and distribution of the SMALPs.
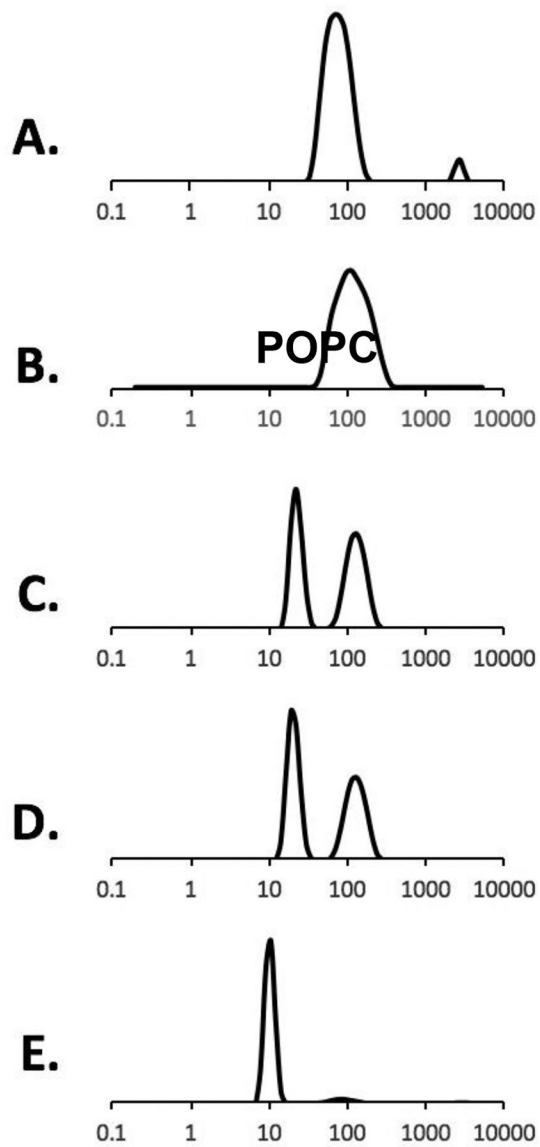
Figure 1.
DLS data showing volume graphs for 2.5 % (m/v) StMA polymer and POPC vesicles. (A) POPC vesicles (control), (B) SMALPs generated from 1:0.5 POPC:StMA, (C) SMALPs generated from 1:1 POPC:StMA, (D) SMALPs generated from1:1.25 POPC:StMA, (E) SMALPs generated from1:1.5 POPC:StMA.
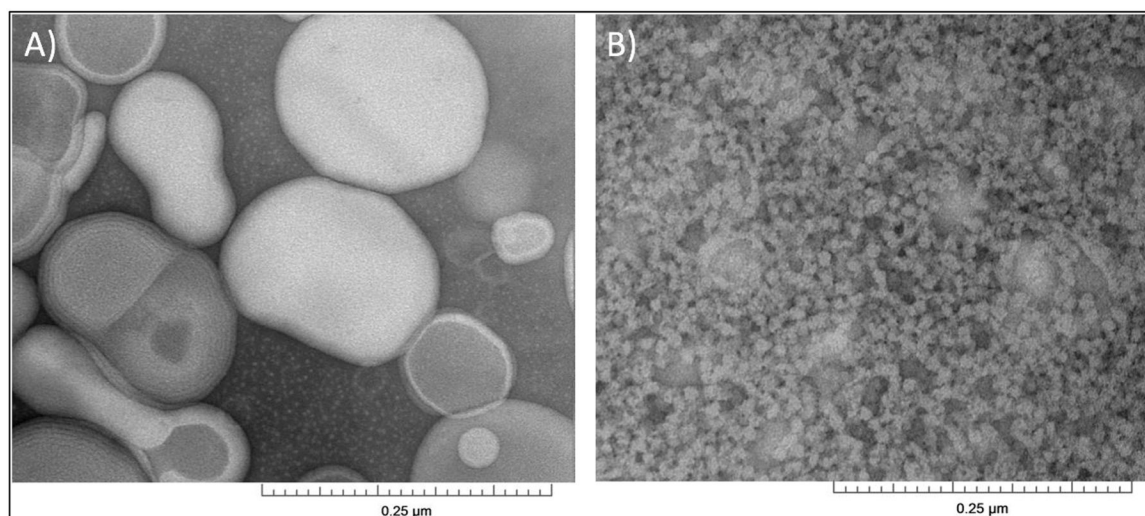
Figure 2.
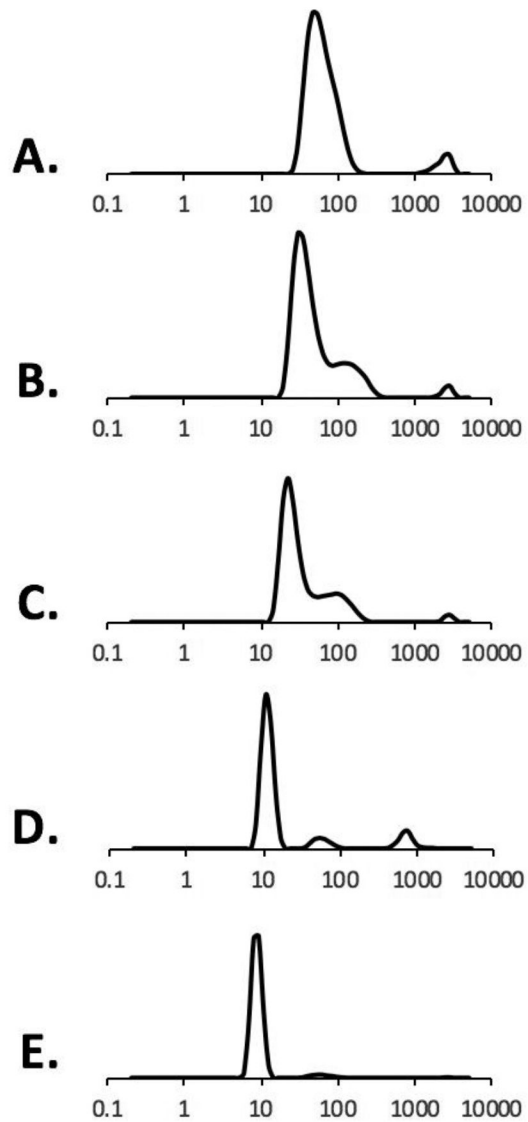TEM micrographs of (A) POPC vesicles (control), and (B) SMALPs generated from 1:1.5 vesicles:StMA.
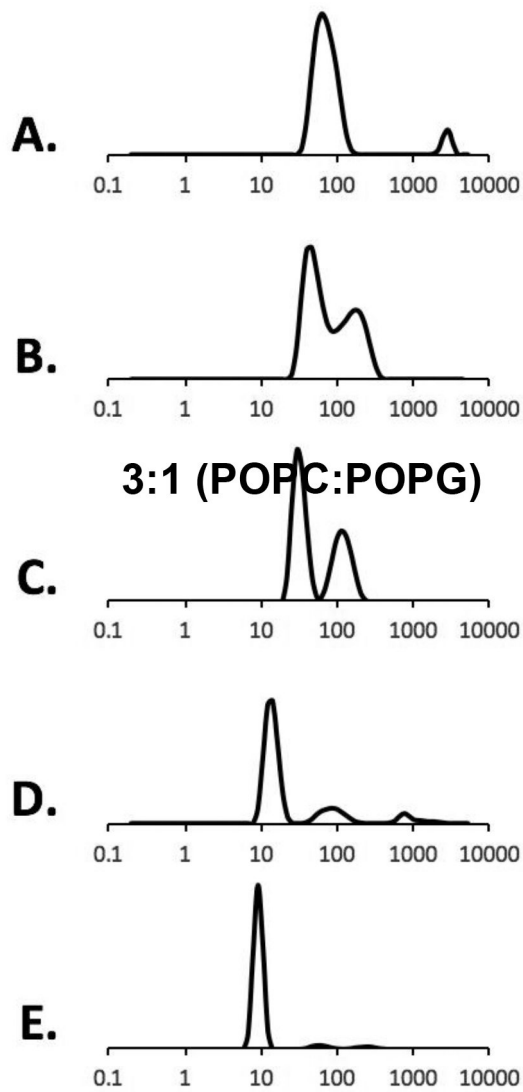
Figure 3.
DLS data showing volume graphs for 2.5 % (m/v) StMA polymer and 3:1 (POPC:POPG) vesicles. (A) POPC:POPG, 3:1 vesicles (control), (B) SMALPs generated from1:0.5 vesicles:StMA, (C) SMALPs generated from 1:1 vesicles:StMA, (D) SMALPs generated from1:1.25 vesicles:StMA, (E) SMALPs generated from1:1.5 vesicles:StMA.
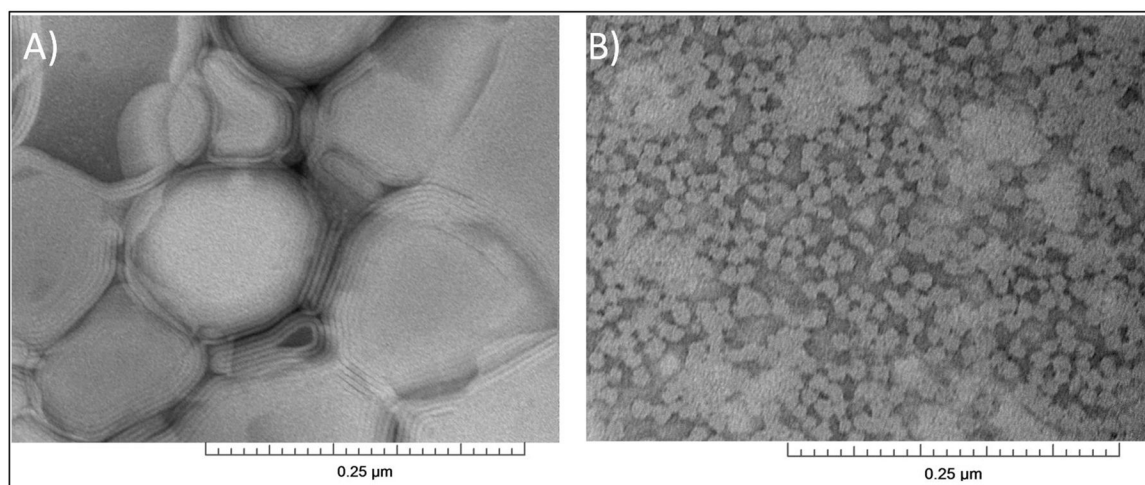
Figure 4.
TEM micrographs of (A) POPC:POPG (3:1) vesicles (control), and (B) SMALPs generated from 1:1.5 vesicles:StMA.

9:1 (POPC:POPG)

Figure 5.
DLS data showing volume graphs for 2.5 % (m/v) StMA polymer and 9:1 (POPC:POPG) vesicles. (A) POPC:POPG 9:1 vesicles (control), (B) SMALPs generated from1:0.5 vesicles:StMA, (C) SMALPs generated from 1:1 vesicles:StMA, (D) SMALPs generated from1:1.25 vesicles:StMA, (E) SMALPs generated from 1:1.5 vesicles:StMA.

Figure 6.
TEM micrographs of (A) POPC:POPG (9:1) vesicles (control), and (B) SMALPs generated from 1:1.5 vesicles:StMA.
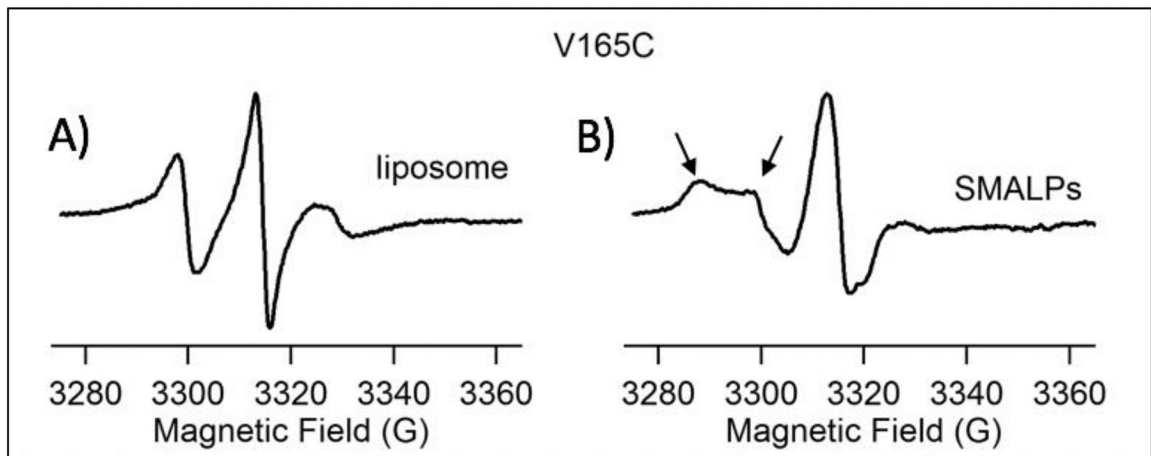
Figure 7.
CW-EPR data on V165C-Q1-VSD mutant in (A) POPC:POPG (3:1) liposomes as control, and (B) SMALPs formed from 1:1.5 (vesicles:StMA), Left arrow shows the slower, rigid limit component of the spin label while the right arrow indicates a faster component.

Table 1

Average particle size distribution of SMALPs resulting from different ratios of vesicles:StMA

	Particle Size (nm)				
Name	**1:0** **(Control vesicles)**	**1:0.5**	**1:1**	**1:1.25**	**1:1.5**
POPC	90	120	21	18	10
3:1 (POPC:POPG)	60	45	30	15	10
9:1 (POPC:POPG)	55	30	21	10	9